VARIATION OF ELECTROMAGNETIC ACOUSTIC TRANSDUCTION SIGNALS WITH MICROSTRESS AND ANISOTROPY IN STEEL PARTS

E. Gorkunov, S. Zadvorkin, A. Makarov, M. Solomein, S. Rodionova
Institute of Engineering Science, Russian Academy of Sciences (Urals Branch), Ekaterinburg, Russia

Abstract: Investigation results on microstresses affecting the parameters of double resonant electromagnetic-acoustic transduction (EMAT) in carbon, low-alloy and high-alloy steels and on the correlation between these parameters and wear resistance under abrasive action and sliding friction in steels with a "fresh" pearlitic structure are presented. The effect of crystallographic anisotropy and the magnetostriction mechanism of excitation of EMAT on its parameters is demonstrated with a monocrystalline Fe-3%Si disk.

Introduction: Due to contactless excitation and easy practical implementation, electromagnetic-acoustic transduction is a promising method for monitoring the stress-strain state. The currently pursued investigations predominantly deal with the effect of external stresses on the EMAT parameters. However, the service properties of materials are substantially governed by microstresses. Therefore investigations into the effect of microstresses on the EMAT characteristics in steels of different classes seem to be of interest.

The paper deals with the effect of microstresses of different level on the parameters of double resonant EMAT in steels, the correlation between these parameters and wear resistance under abrasive action and sliding friction, and the effect of crystallographic anisotropy and magnetostriction mechanism on the EMAT signal in a monocrystalline Fe-3%Si disk.

Results: Samples of the carbon steels 25 (C≅0,24%), 70 (C≅0,70%) and U8 (C≅0,80%), the low-alloy carbon steel ShH15 (C≅0,98%; Cr≅1,38%; Mn≅0,32%), the high-alloy high-carbon steel R6M5 (C≅0,84%; Cr≅3,30%; W≅5,92%; V≅1,80%; Mo≅4,83%), the austenitic-martensitic low-carbon nitrogen steel 13H15N5AM3Sh (C≅0,14%; Cr≅15,5%; Mn≅0,49%; Ni≅4,37%; Mo≅2,40%; N≅0,50%) and the carbon steel U9 (C≅0,94%) were studied. Different levels of microstresses in the samples were obtained by the variation of thermal treatment conditions (steels U8, U9, ShH15, R6M5, 13H15N5AM3Sh) or cold plastic deformation (patented steels 25 and 70).

The samples of the steels U8, ShH15, 13H15N5AM3Sh and R6M5 were quenched and then tempered. After thermal treatment, the samples were ground and subjected to electrolytic finishing in order to eliminate the influence of mechanical working on microstresses. The samples of the carbon steel U9 were heated up to 1050°C and put into a salt bath. At a temperature of 500°C in the bath and holding for 1 min, with further cooling in water, the initial fine pearlitic structure was obtained in the steel. Then some of the samples were annealed at 600°C (the duration of holding in the salt bath was varied between 2 and 600 min), with further cooling in water.

Wire samples of steels 25 and 70 were patented under the following conditions: heating in a continuous furnace up to 900°C, cooling in a salt bath to 500°C, holding at this temperature for 30 seconds and air cooling. Then the samples were subjected to cold deformation by drawing through dies. The maximum degree of deformation was 99,2% for steel 25 and 96,3% for steel 70, the sample diameter varying from 2,6 mm in the initial state to 0,225 mm (steel 25) and to 0,50 mm (steel 70).

The effect of crystallographic anisotropy on the EMAT parameters was studied on a monocrystalline Fe-3%Si disk. The disk plane was deflected from the crystallographic plane {110} through $\beta \approx 2°$.

X-ray studies were conducted on a diffractometer with the use of K_α-radiation of chromium for steels U8, ShH15, R6M5, 25, 70 and 13H15N5AM3Sh and Fe-K_α-radiation for steel U9. The microstresses and the typical dimension of the coherent scattering regions D were estimated by the $K_{\alpha 1}$-component of line (211) of the α-phase, and for steel U9 – by the $K_{\alpha 1}$-component of line

(110). Note that it is lattice microdistortions ε, not microstresses, that are determined by the X-ray analysis, therefore the paper presents data on ε.

The abrasive resistance of steels was studied on the sliding of sample faces on an emery paper. Wear resistance was defined as a ratio between the mass loss of the standard sample (armco-iron) and the mass loss of the material being tested taken from three concurrent tests. Sliding friction wearing tests were conducted on a laboratory installation by a pin-plate scheme, in the atmosphere, dry. Wear rate was calculated by the formula $Ih=\Delta m/\rho SL$, where Δm is sample mass loss; ρ is sample material density; L is rubbing path; S is geometric contact area. Wear resistance was determined by the results of three tests.

The amplitude E of the EMAT signal at resonance and elastic wave velocity V was measured by passage-type sensors. The zero symmetric mode of longitudinal normal elastic waves was used. The external constant polarization magnetic field H_{opt} created by an electromagnet and directed along the sample axis, was selected for each sample by the maximum value of E. This maximum was observed in the region of the rotation of the spontaneous magnetization vectors at the polarization field corresponding to the magnetic induction region 0,7 to 0,9 of induction of saturation.

The effect of crystallographic anisotropy on the EMAT parameters was studied on monocrystalline Fe-3%Si, which was discretely rotated in the polarization H_{opt} and excitation H_b fields through the angles α about the easy direction of magnetization coinciding with the crystallographic direction [001]. The field dependences of the longitudinal $\lambda_{||}$ and lateral $\lambda_{\perp}$ magnetostriction for the disk were measured by the tensometric method at various α.

Discussion: The quantities ε, D, E and V as dependent on the tempering temperature T_{temp} are shown in fig.1. It is obvious that the value of ε decreases monotonically and the values of D, E and V increase as T_{temp} of steels U8 and ShH15 rises. This is due to the disintegration of martensite and retained austenite, the isolation of carbon from the α-solid solution, the decrease in the dislocation density.

In the high-alloy high-speed steel R6M5 the processes of the disintegration of martensite and retained austenite are displaced to the region of higher temperatures – between 480°C and 550°C. Therefore slight variations in the EMAT parameters at low and medium tempering temperatures are associated with some isolation of carbon from the α-solid solution. The main variations on the dependences $\varepsilon(T_{temp})$, $D(T_{temp})$, $E(T_{temp})$ and $V(T_{temp})$ occur at temperatures above 480°C. They are caused by the disintegration of martensite and retained austenite (and hence a more conspicuous isolation of carbon from the α-solid solution), lower magnitude of microdistortions and greater regions of coherent scattering. These processes are accompanied by higher EMAT signal amplitude and elastic wave velocity. The formation of special fine-disperse chromium carbides at temperatures from 480°C to 520°C leads to a slightly higher level of microstresses due to the appearance of dispersion stresses. This process is accompanied by modest extremes on the curves $\varepsilon(T_{temp})$, $D(T_{temp})$, $E(T_{temp})$ and $V(T_{temp})$.

At tempering temperatures below 400°C the dependences $\varepsilon(T_{temp})$, $D(T_{temp})$, $E(T_{temp})$ and $V(T_{temp})$ for samples of the corrosion-resistant austenitic-martensitic steel 13H15N5AM3Sh have the same behavior as for samples of other steels, see fig.1. However, the EMAT signal amplitude decreases at temperatures above 400°C. This is due to the isolation of fine-disperse chromium carbonitride from martensite at tempering temperatures above 400°C and the inverse $\alpha \rightarrow \gamma$ transformation within the range between 600°C and 650°C [1]. Tempering at temperatures from 650°C to 700°C is accompanied by austenite disintegration, and, as a result, the EMAT amplitude increases again.

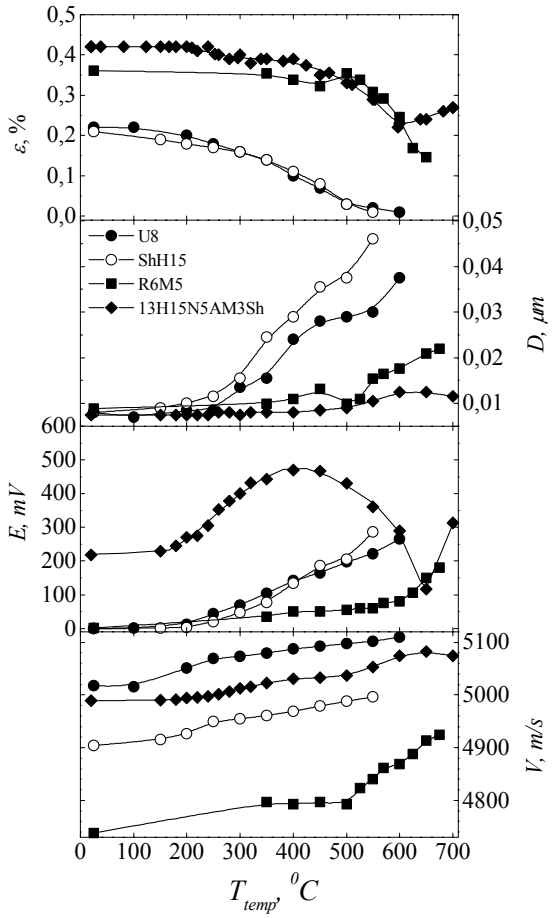

Fig.1. Microdistortions ε, typical dimension of coherent scattering regions D, EMAT amplitude E and elastic wave velocity V as dependent on tempering temperature T_{temp} for steels U8, ShH15, R6M5, 13H15N5AM3Sh.

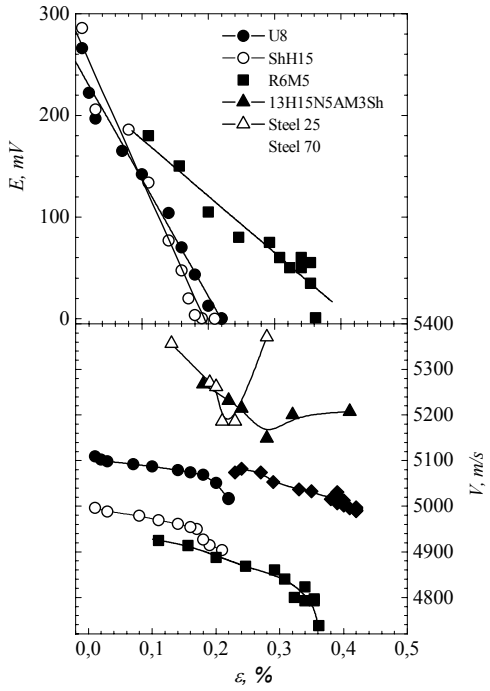

Fig.2. EMAT amplitude E and elastic wave velocity V as dependent on microdistortions ε for steels 25, 70, U8, ShH15, R6M5, 13H15N5AM3Sh.

Fig.2 shows the EMAT signal amplitude and the elastic wave velocities as dependent on lattice microdistortions for heat-treated steels. For the steels U8, ShH15 and R6M5, the value of E is seen to decrease linearly as microdistortions grow. In the steel 13H15N5AM3Sh having the highest concentration of alloying elements among the steels studied, the EMAT signal amplitude is nonmonotonically related to lattice distortions, since it grows at tempering temperatures below ≈400°C and then decreases until the tempering temperatures reach 650°C. Thus, for this high-alloy steel, the resonance EMAT amplitude cannot serve as a parameter for monitoring microstresses within the whole range of tempering temperatures.

The dependences E(ε) for deformed steels differ from linear, especially for samples of steel 70. However, it should be noted that the curves E(ε) deviate from linearity at lattice microdistortions over 0,2% (this corresponds to the degree of deformation over 60%), i.e., greater than microdistortions in heat-treated carbon and low-alloy steels. At lower values of ε, the EMAT signal amplitude in deformed steels, as in most heat-treated steels, decreases linearly with the growth of lattice microdistortions. In heat-treated steels, including steel 13H15N5AM3Sh, the elastic wave velocity decreases monotonically with the growth of lattice microdistortions. For cold-deformed steels, the initial stage of deformation also shows monotonic decrease in V with the growth of microdistortions and then, due to decreasing angle of dispersion of the crystallographic texture in drawing, the velocity of acoustic waves increases.

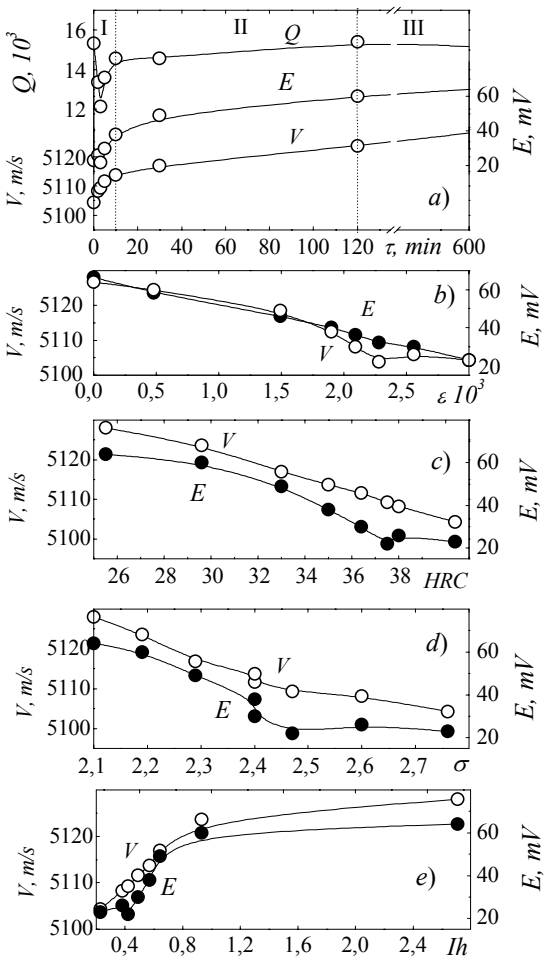

Fig.3. EMAT amplitude E, elastic wave velocity V and the EMAT signal quality factor Q as dependent on the duration of annealing τ at 650℃ (a); EMAT signal amplitude E and sound velocity V as dependent on microdistortions ε (b), hardness HRC (c) and wear resistance σ (d), wear rate Ih (e) for steel U9.

Fig.3 presents physical-mechanical properties, α-phase lattice microdistortions, magnetic, electromagnetic characteristics and EMAT parameters for steel U9 as dependent on the duration of annealing τ at 650°C. As microstresses decrease, the EMAT signal amplitude, the quality factor Q and the velocity of the longitudinal elastic wave V must rise with the increasing duration of annealing [2]. It is obvious from fig.3a that V actually increases as the duration of annealing grows. At the same time, at short annealing (τ≤3 min), the EMAT signal amplitude remains constant within the limits of the measurement error, whereas the value of the quality factor Q decreases almost by 25 % and reaches its minimum at τ=3min. It is only at more durable annealing that E and Q increase. This behavior of the dependences E(τ) and Q(τ) in zone I must be caused by the additional influence of carbon redistribution. Note that the most sensitive to these processes among the parameters is the EMAT signal quality factor.

In the annealing duration intervals from 10 to 120 min (zone II) and from 120 to 600 min (zone III) the EMAT parameters for steel U9 exhibit a quieter variation than in zone I, see fig.3a. When the duration of annealing is more than 10 min, the α-phase lattice microdistortions decrease continuously, in the polygonization and recrystallization develop in the magnetic core matrix, and the carbide phase demonstrates spheroidization (zones II and III), coagulation and coalescence (zone III). These structural changes are responsible for a gradual increase in the values of V, E and Q, which can be seen in fig.3a.

It follows from fig.3(b-e) that most durations of annealing exhibit a single-valued relations of sound velocity V and amplitude E to hardness HRC, abrasive resistance σ, wear rate Ih at sliding friction and α-phase lattice microdistortions ε (see fig. 4b-e), excluding short holding (τ≤3 min).

At $\tau \leq 3$ min, a spread of the EMAT signal amplitude E is observed. As distinct from the above-mentioned characteristics, the quantity V may be viewed as a check parameter applicable to any duration of holding, including minimal, i.e. 2 to 3 min, see fig.3a. Note the linear behavior of the V – HRC and V – ε relationship, see fig. 4b,c.

It follows from the investigations that the EMAT method is highly sensitive to the elimination of excess carbon in ferrite and lower damage of cementite occurring in short annealing of steels with the initial structure of thin pearlite. Therefore longitudinal sound wave velocity V measured by the EMAT method is an effective parameter to be used for inspecting the presence of the unbalanced structure of "fresh" fine pearlite in steels, which exhibits maximum hardness and wear resistance in steels.

Fig. 4a presents results of measurements of longitudinal $\lambda_{\parallel}$ and lateral $\lambda_{\perp}$ magnetostriction in fields corresponding to maximum E for a monocrystalline Fe-3%Si disk at different values of α. When the direction of the polarization field coincides with the sample axis [001] (α=0°), longitudinal magnetostriction peaks, $\lambda_{\parallel} \approx 20{,}7 \cdot 10^{-6}$, and lateral magnetostriction reaches its minimum, $\lambda_{\perp} \approx -11{,}7 \cdot 10^{-6}$. This is due to a great volume of 90° magnetic phases, as the disk plane diverged from the crystallographic plane {110} through $\beta \approx 2°$. When β=0°, longitudinal magnetostriction $\lambda_{\parallel}$ would normally have a minimum value at α=0° [3].

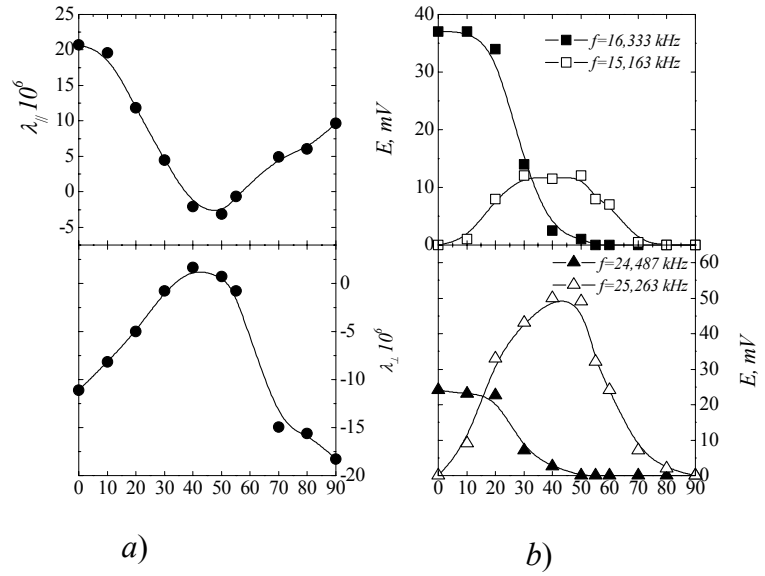

Fig.4. Longitudinal $\lambda_{\parallel}$ and lateral $\lambda_{\perp}$ magnetostriction corresponding to the maximum EMAT signal amplitude (a) and EMAT signal amplitude for different resonant frequencies (b) as dependent on the angle α between the easy direction of magnetization [001] of a monocrystalline Fe-3%Si disk and the direction of the polarization magnetic field H_{opt}.

At different frequencies of the excitation magnetic field, the EMAT signal amplitude becomes noticeable only at the polarization field values that provide magnetic induction of ~ 1,5 to 1,7 T. When the amplitude-frequency characteristic of the EMAT signal is measured on a monocrystalline disk, a spectrum of EMAT signals was obtained. It appears that the dependences E(α) may be of two types – E is maximal when α=0° or when $\alpha \cong 55°$. That is, the EMAT signal amplitude is maximal when the polarization field is directed along the crystallographic axis [001] for the dependences E(α) of one type and along the axis [111] for the dependences of the other type. Fig.4b presents the dependences E(α) for some resonant frequencies as examples. A comparison between fig. 4a and fig.4b

shows that the behavior of the dependence $E(\alpha)$ of type I is similar to that of the dependence $\lambda_{\parallel}(\alpha)$, whereas the dependence $E(\alpha)$ of type II behaves similarly to the dependences $\lambda_{\perp}(\alpha)$. It can therefore be

supposed that the EMAT signal spectrum is formed of the modes of two types, one of which is predominantly affected by the longitudinal component of magnetostriction, the other being influenced by the lateral component.

Conclusions: The amplitude of the signal of electromagnetic-acoustic transformation in carbon, low-alloy and high-alloy steels decreases practically linearly as lattice microdistortions caused by heat treatment grow. The exception is the high-alloy corrosion-resistant austenitic-martensitic steel 13H15N5AM3Sh, which exhibits a non-single-valued relation of EMAT signal amplitude to microdistortions. As distinct from the EMAT signal amplitude, all the steels studied, including 13H15N5AM3Sh, demonstrate a single-valued relation of normal elastic wave velocity to lattice microdistortions caused by heat treatment. Thus, it is possible to use EMAT parameters for estimating microstresses occurring in steels due to heat treatment. For cold-deformed steels, this estimation is possible only with the degree of deformation under 60%.

The EMAT method is highly sensitive to structural changes taking place under short annealing in high-carbon steels with a thin pearlitic structure. Single-valued relations of V and E to hardness, wear resistance and internal microstresses have been revealed.

The work has been partially done with a support from the Russian Foundation for Fundamental Research, grant 03-01-00794.

References: 1. Voznesenskaya, N.M., Izotov, V.I., Ulyanova, N.V., Popova, L.S., Potak, Ya.S. The structure and properties of high-strength stainless steel 1H15N4AM3. – Metallovedenie I Termicheskaja Obrabotka Metallov, 1978, №1, p.32 – 35 (in Russian).

2. Bobrenko,V.M., Averbukh, I.I. A study of stresses with the application of EMA transducers. - Defektoskopiya, 1971, № 3, p. 132 –134 (in Russian).

3. Zaikova, V.A., Shur, Ya.S. The behavior of magnetostriction curves of silicon iron crystals as dependent on the behavior of the domain structure under magnetization. – Fizika Metallov I Metallovedenie, 1964, 18. p. 349 – 358 (in Russian).